SUPPORTING INFORMATION

Real-time analysis of porphyrin J-aggregation on a plant-esterase-functionalized surface using quartz crystal microbalance with dissipation monitoring

Limin Yang[a], Lei Jiang*[,a], Weijing Yao[b,c], Junling Liu [a], and Juan Han[a]

[a]State Key Laboratory of Heavy Oil Processing and Center for Bioengineering and Biotechnology, China University of Petroleum (East China), Qingdao, Shandong 266555, P. R.

[b]China Evidence Identification Center, Chongqing Municipal Public Security Bureau, Chongqing 400021, P. R.

[c]China Chongqing Municipal Engineering Research Center for Criminal Investigation, Chongqing 400021, P. R. China

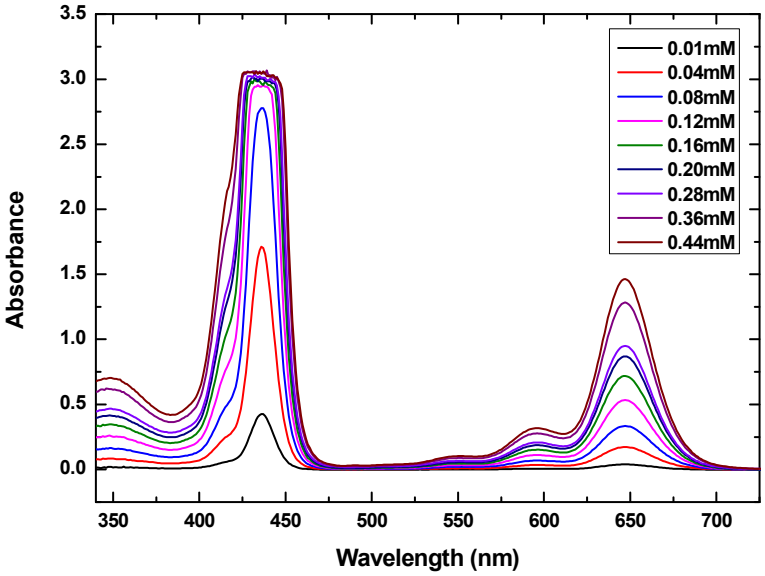

Figure S1. Absorption spectra of initial $TPPS_4$ solutions used for QCM-D measurements. The absorption spectra were collected immediately after the preparation of samples with Shimadzu UV-2450 spectrophotometer using 0.1 cm path length quartz cuvette.

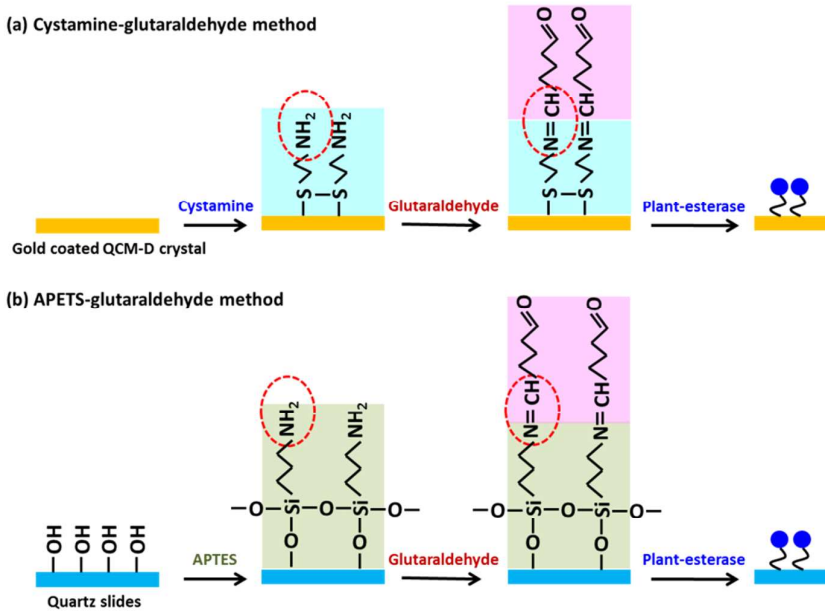

Figure S2. The surface modification procedure involved in plant-esterase immobilization on (a) QCM-D gold chip and (b) quartz slides.

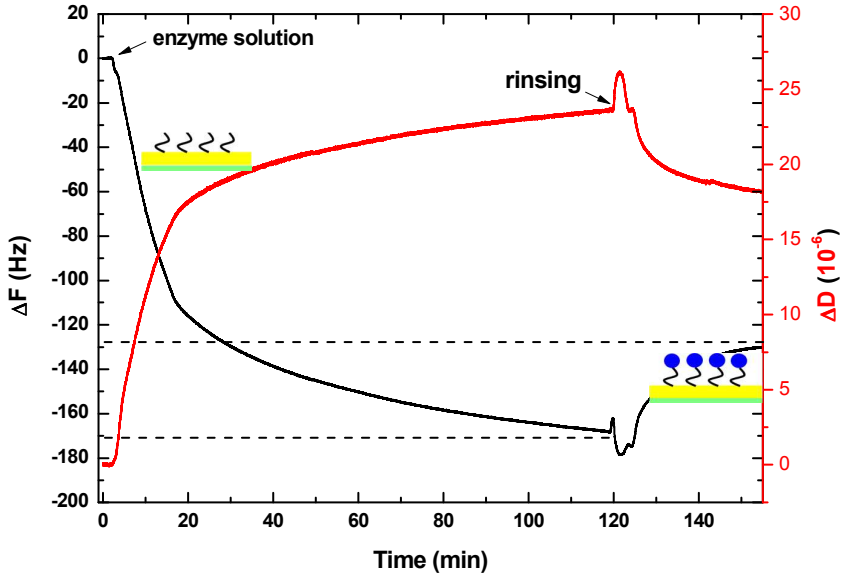

Figure S3. All the signal frequency and dissipation variation during plant-esterase immobilization process. It was detected a frequency variation of about -129.7 Hz for plant-esterase immobilization process. From this value and using Voigt model, the mass of plant-esterase immobilized in the self-assembled monolayer of cystamine over the quartz crystal surface was inferred to 54.27 mg m^{-2}. The analysis assumed a density of 1000 kg m^{-3} for the immobilized layer.

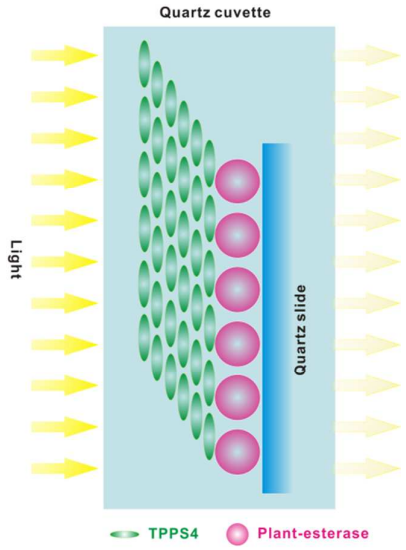

Figure S4. Schematic presentation of the spectroscopic measurements using UV/vis absorption, fluorescence, RLS and CD spectroscopies.

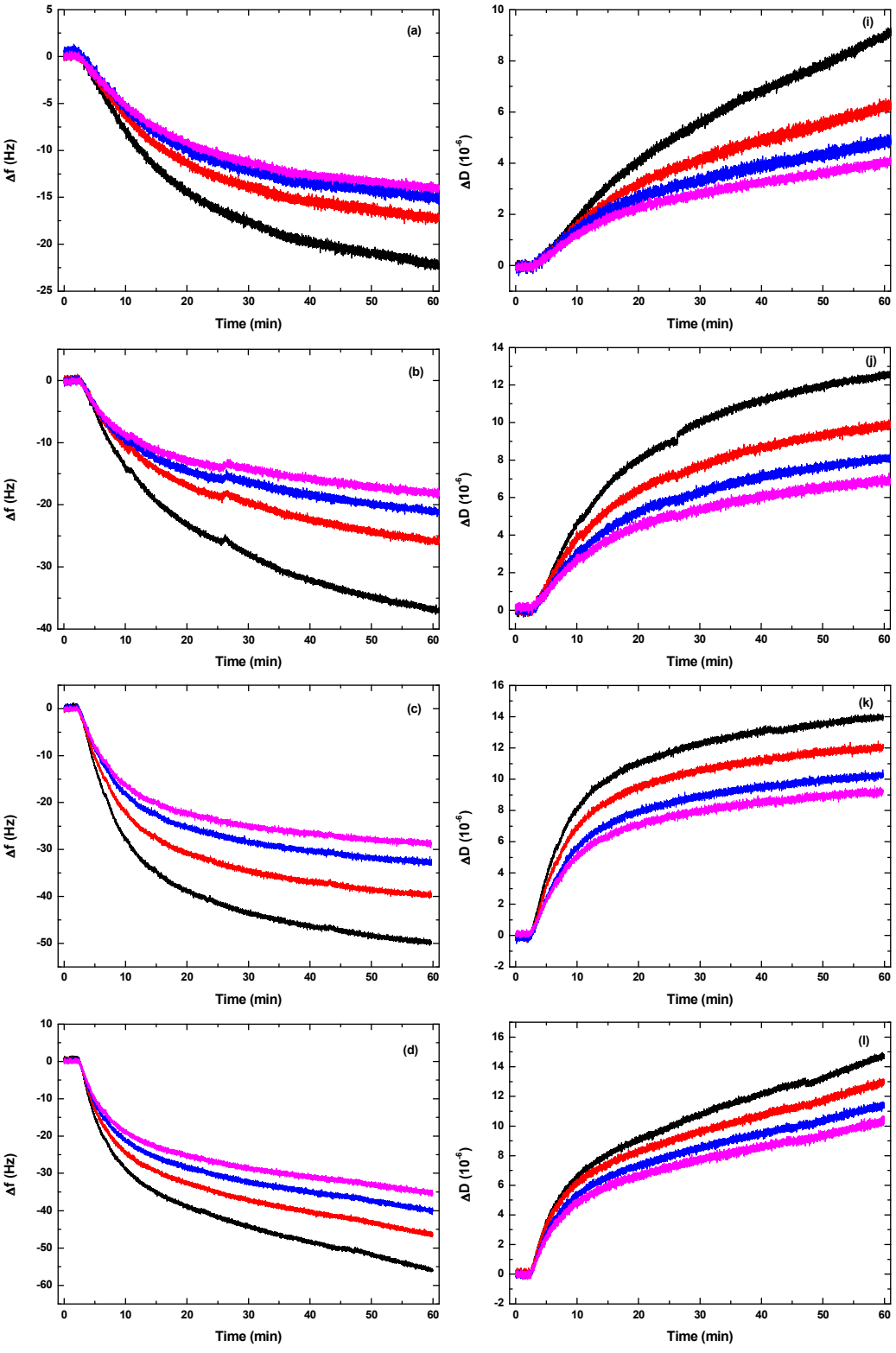
(a)
(b)
(c)
(d)
(i)
(j)
(k)
(l)
Δf (Hz)
ΔD (10⁻⁶)
Time (min)

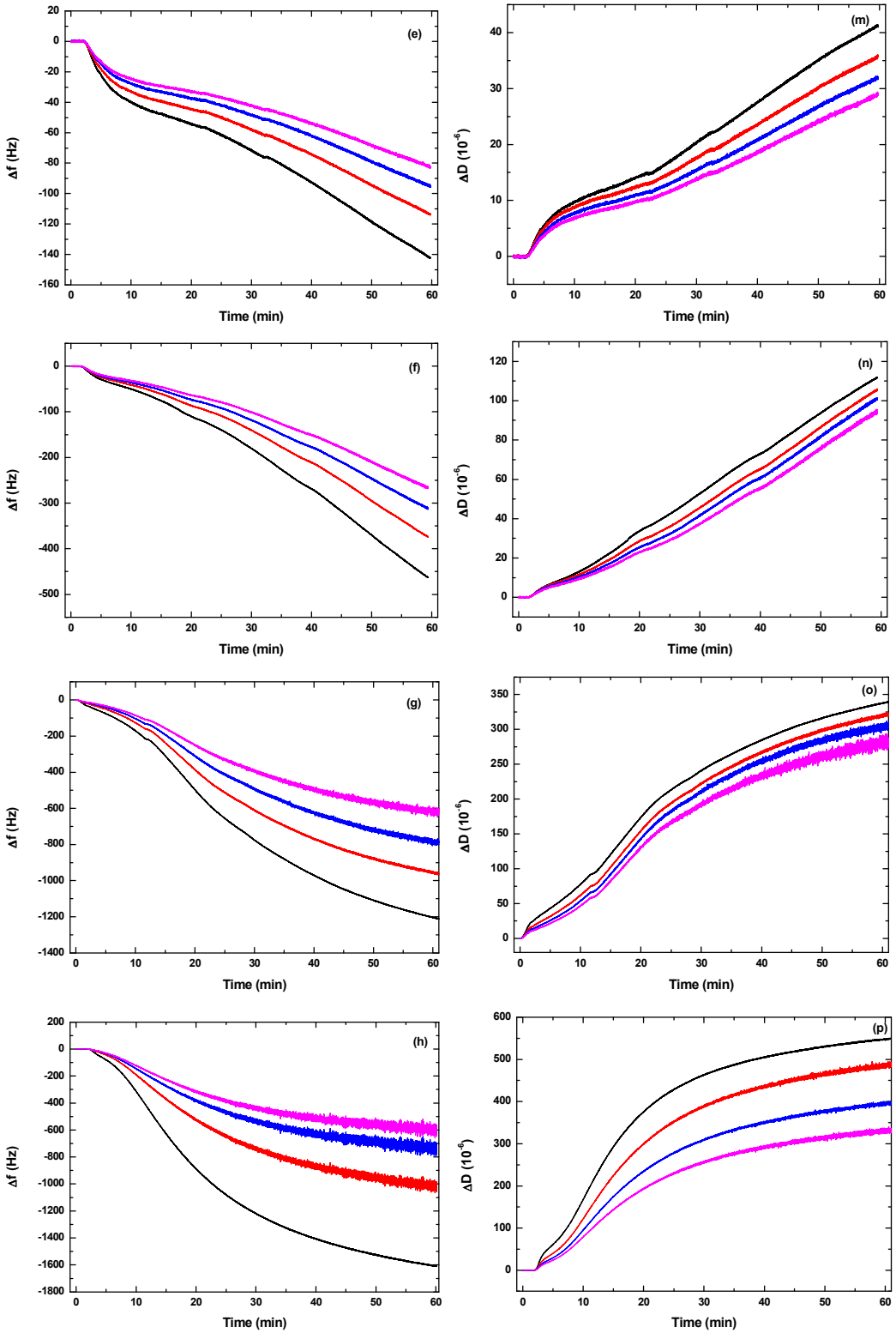

Figure S5. Changes in f (a-h) and D (i-p) during adsorption of $TPPS_4$ at eight different concentrations: 0.01mM (a and i), 0.04 mM (b and j), 0.08 mM (c and k), 0.12 mM (d and l), 0.16 mM (e and m), 0.20 mM (f and n), 0.28mM (g and o), and 0.36mM (h and p), at four different frequency overtones: (black) 3rd, (red) 5th, (blue) 7th, and (pink) 9th.

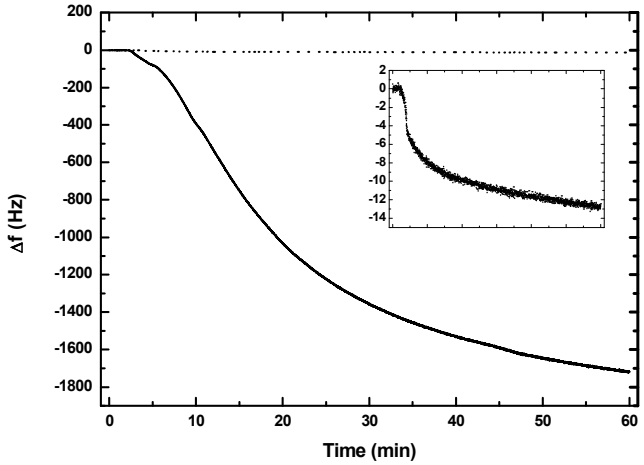

Figure S6. Comparison of $TPPS_4$ adsorption in acidic medium (pH 1.38, line) with that in neutral medium (pH 7.0, points). [$TPPS_4$] = 0.44 mM. Inset: expanded view of the points.

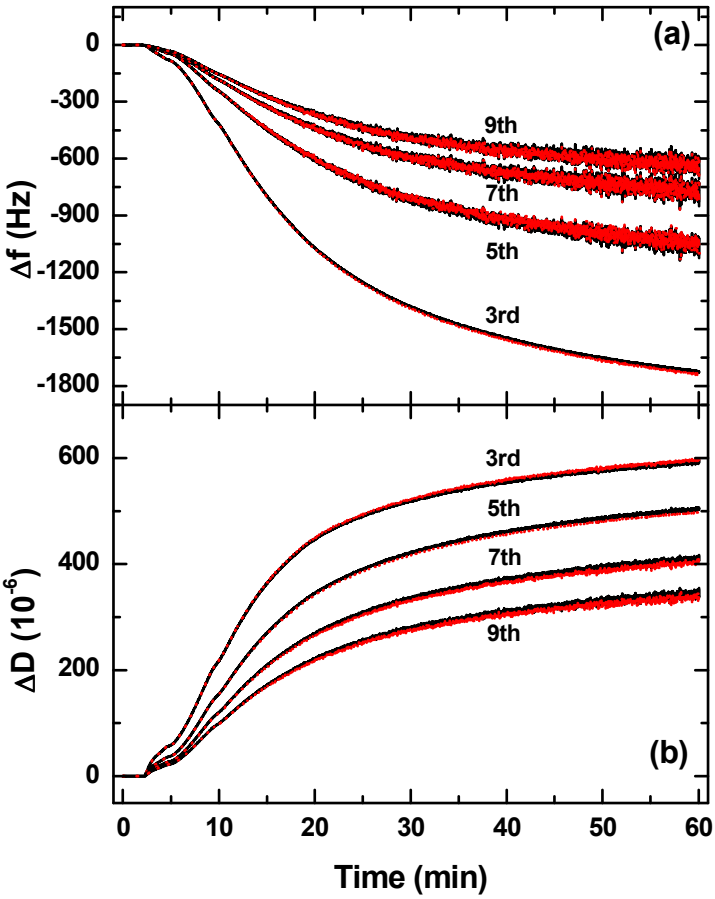

Figure S7. Voigt viscoelastic model fitting. Δf (a) and ΔD (b) versus time at n=3rd, 5th, 7th and 9th overtones for the $TPPS_4$ adsorption are shown as black lines. The best fit between the data and the Voigt viscoelastic model is shown as red points. [$TPPS_4$]= 0.44 mM.

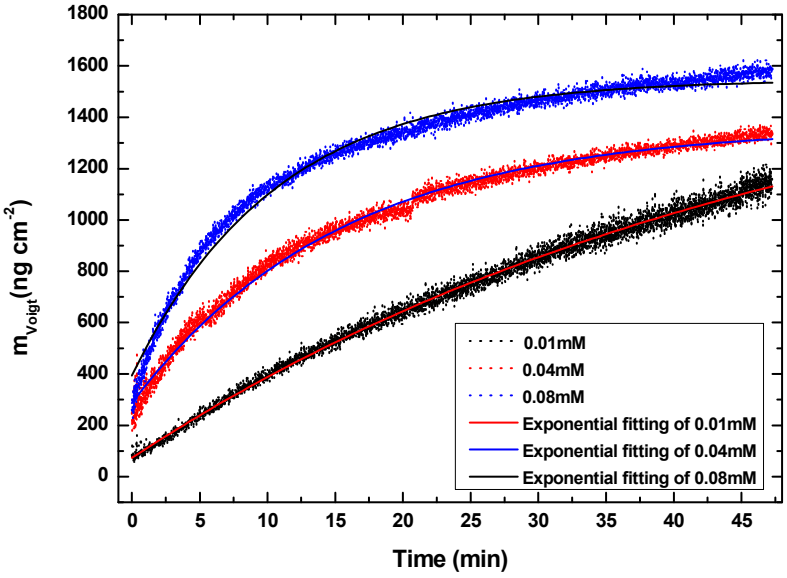

Figure S8. Curve fitting for experimental points (dots) and fitted curve for the proposed mathematical equation defining $TPPS_4$ aggregate nucleation (line).

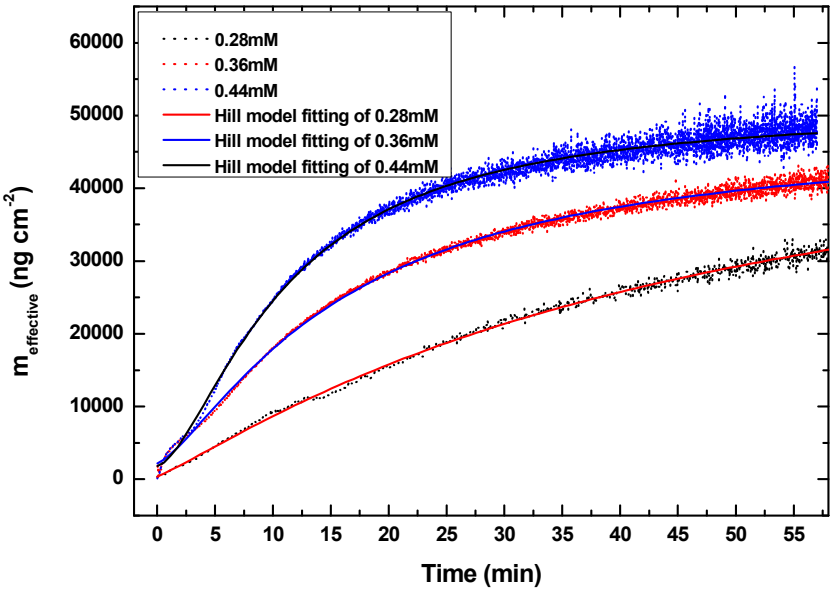

Figure S9. Curve fitting for experimental points (dots) and fitted curve for the proposed mathematical equation defining $TPPS_4$ aggregation (line).

Table S1. Boundary conditions employed for analysis of QCM-D data using Voigt model.

$[TPPS_4]$ (mM)	0.01	0.04	0.08-0.20	0.28-0.44
Viscosity (kg m^{-1} s^{-1})	0.001-0.01	0.0005-0.01	0.0005-0.01	0.0005-0.01
Shear (Pa)	1×10^{4}-1×10^{6}	1×10^{4}-1×10^{8}	1×10^{4}-1×10^{8}	1×10^{4}-1×10^{8}
Thickness (m)	1×10^{-10}-1×10^{-6}	1×10^{-8}-1×10^{-6}	1×10^{-10}-1×10^{-6}	1×10^{-7}-1×10^{-3}
Mass (ng cm^{-2})	1×10^{3}-1×10^{5}	1×10^{3}-1×10^{5}	10-1×10^{5}	10-1×10^{7}

Table S2. First-order kinetic parameters (Eq. 1) obtained for $TPPS_4$ aggregate nucleation on the plant-esterase-functionalized QCM-D surface at pH 1.38.

$[TPPS_4]$ (mM)	τ (min)	R
0.01	49.55±0.36	0.9969
0.04	15.41±0.05	0.9961
0.08	10.61±0.03	0.9935
0.12	7.82±0.08	0.9942
0.16	5.93±0.03	0.9977
0.20	4.35±0.04	0.9982
0.28	3.01±0.20	0.9950
0.36	1.44±0.03	0.9947
0.44	1.41±0.02	0.9965

Table S3. Aggregation parameters (Eq. 2) calculated from frequency data for the plant-esterase-functionalized QCM-D surface with $TPPS_4$ at pH 1.38.

$[TPPS_4]$ (mM)	k (min)	n	R
0.28	46.43±0.48	1.13±0.006	0.9986
0.36	16.00±0.03	1.35±0.004	0.9985
0.44	11.07±0.03	1.56±0.006	0.9974